

An Application of a New X-ray Diffraction System with Imaging Plates to Studies on the Deformation Behavior of Ultra-high Molecular Weight Polyethylene.

Akiyoshi KAWAGUCHI*, Shozo MURAKAMI*, Ken-ichi KATAYAMA*,
Masahiko MIHOICHI** and Toshihiko OHTA***

Received June 28, 1991

An X-ray diffraction system with imaging plates was built so that a time series of X-ray diffraction patterns were recorded at intervals of a short time. With the system, the deformation behavior of ultra-high molecular weight polyethylene was studied dynamically. Drawn at room temperature, the ultra-high molecular weight polyethylene was oriented exhibiting the monoclinic phase, but was not drawn into a fiber structure even when it was drawn till broken. On drawing it at high temperatures above 85°C, it transformed into a fiber structure without producing the monoclinic phase.

KEY WORDS: Imaging plate / X-ray diffraction / Ultra-high molecular weight polyethylene / Drawing / Monoclinic phase / Orthorombic phase/

INTRODUCTION

Nowadays, high power X-ray sources by rotating anode X-ray generator and synchrotron are available for diffraction work, and various high performance X-ray intensity detectors such as a PSPC(position sensitive proportional counter) and an X-ray TV system are developed. In combination with a high power X-ray source and a highly sensitive X-ray detector, an X-ray diffraction pattern is able to be quickly taken for a very short time, even shorter than 1 sec. Thus, a sequence of X-ray diffraction patterns can be recorded at intervals of a very short time, while the structure of crystalline polymer solids is being changed or re-organized. For example, by using a PSPC system combined with a rotating anode X-ray generator, we measured the thickening rate of polyethylene single crystals during heat-treatment and showed that when the heating rate is low, they thicken through sliding diffusion of molecular chains along their stems.¹⁻²⁾ Measuring the change of lamellar thickness of solution-grown polypivalolactone crystals during heating at a constant rate, we also elucidated that they re-organize by repetition of remelting and recrystallization until final melting.³⁾ Further, we rapidly recorded X-ray diffraction patterns by an X-ray TV

*) 河口 昭義, 村上 昌三, 片山 健一: The Institute for Chemical Research, Kyoto University, Uji, Kyoto 611

**) 三歩一 真彦: Toyobo Co. Ltd., Katada, Shiga 520-02

***) 太田 利彦: Faculty of Living and Science, Osaka City University, Sumiyoshi-ku, Osaka 545

system while polyethylene was being drawn, and found that polyethylene transforms into a fiber structure of the orthorhombic phase, the monoclinic phase being transiently produced in the process.^{4,5)} Though both systems thus are of advantage to dynamical studies on the structural changes of crystalline materials, either of both suffers from drawbacks; the PSPC counts X-rays rapidly and quantitatively but its suitable application is limited to the case of one-dimensional measurement because losses in counts are significant at high intensity, and the X-ray TV system is very powerful in recording extremely rapidly the X-ray diffraction patterns on a video tape recorder but cannot measure quantitatively the diffraction intensity. Recently, a new medium for recording X-ray intensities quickly and quantitatively, the imaging plate (IP), was developed and utilized for X-ray diffraction work.⁶⁻⁸⁾ The IP has advantages of covering a wide dynamic range of intensity and of taking a two-dimensional pattern without counting losses.

So far, mechanical deformation behavior of polyethylene was studied in terms of deformation of spherulites using X-ray diffraction,^{9,10)} and optical and electron microscopy.^{11,12)} Recently, the real-time studies on drawing melt-crystallized ultra-high molecular weight polyethylene (UHMWPE) were performed in combination of the intense radiation from an rotation anode X-ray generator⁵⁾ or synchrotron^{13,14)} with an X-ray TV system. We developed a new X-ray diffraction system with the IP. In the present paper, the performance of the IP X-ray system and some results obtained by applying it to the study on the large deformation of UHMWPE are described.

EXPERIMENTAL

Apparatus

Phosphors with the chemical formula of $\text{BaFX}:\text{Eu}^{2+}\text{S}^{2-}$ ($\text{X}=\text{Cl}, \text{Br}, \text{I}$) are photostimulated to emit luminescence. When these photostimulable phosphors are irradiated with X-rays, they are capable of storing a fraction of their energy to excite the color centers called F-center. When illuminated by visible light, the excited phosphors emit luminescence (photostimulated luminescences (PSL)) whose intensity is proportional to the stored energy of irradiated X-rays. Thus, the photostimulated-luminescent materials can be utilized as an area medium of measuring X-ray intensities quantitatively. Further, the IP is superior to X-ray photographic films in that it can be cyclically used because the photostimulated luminescent property is not damaged by repeating the excitation and emission. The IP is a flexible polymer plate which is coated with fine crystalline powder of the phosphors in a thin layer of the thickness of 0.15mm. The IP is commercially produced by Fuji Film Co. Ltd.

In cooperation with MAC Science Co. Ltd., we constructed a new apparatus with the IP so that a sequence of X-ray diffraction patterns could be recorded during the structural change of crystalline polymer solids, for example, by heating or drawing, as sketched in Fig. 1. Now, Fuji Film Co. Ltd. monopolizes the production of the IP, and hence, severe restrictions to use the IP is imposed; the IP is not allowed to be detached from the apparatus and to be moved to other places for reading out intensity data. We were forced to build in devices of recording and reading out intensities as a set.

New X-ray Diffraction System with Imaging Plates

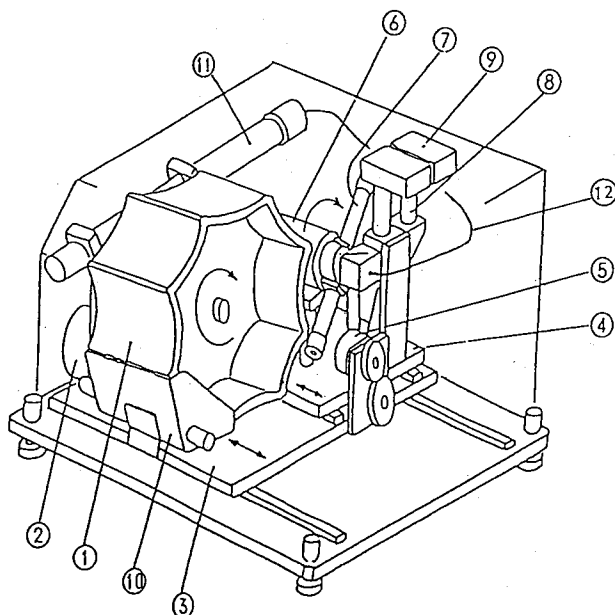


Fig. 1 Sketch of an Ip X-ray recording apparatus with a octahedral drum (cited from the pamphlet issued by MAC Science Co. Ltd.).

1. Imaging Plate (IP) and the cassette with Ips.
2. Pulse motor to drive the IP cassette.
3. Stage on which the IP cassette is set, sliding from side to side.
4. Stage on which the device for reading out the intensity data is set.
5. Pulse motor to drive the data-reading stage.
6. Motor to rotate the reading device.
7. Optical tube for focusing the laser beam on and measuring the emitted PSL from the IP.
8. Photo-multiplier.
9. Pre-amplifier.
10. Lamp for returning the IPs to the ground state.
11. He-Ne gas laser.
12. Optical fiber.

Accordingly, an IP cassette with a polyhedral drum, a hexagonal one in our case, was designed as follows. All six faces of a hexagonal drum are concaved with the curvature of 150mm, and IPs are adhered to the faces. The drum can rotate around and shift along its axle. By controlling the rotation and shift of the drum using a personal computer, different IPs and different areas of an IP can be selected to be exposed for a given period of time. Thus, many X-ray diffraction patterns are recorded on the drum in sequence. Since a rotating anode X-ray generator (Rigaku Ru-300 operated at 40kV -240mA) was used as an X-ray source, an X-ray diffraction pattern giving reliable intensity data could be taken up for a few seconds at the largest rate possible. Thus, X-ray diffraction patterns could be sequentially recorded with an exposure time of 5 secs.

The intensity data of exposed IPs are read out by illuminating the IPs with a He-Ne gas laser ($\lambda = 632.8\text{nm}$). To speed up read out of intensity data, scanning the IP by laser beams is devised in the following way: an optical device focusing laser beams on and measuring the emitted PSL intensities from the IP is designed in the form of

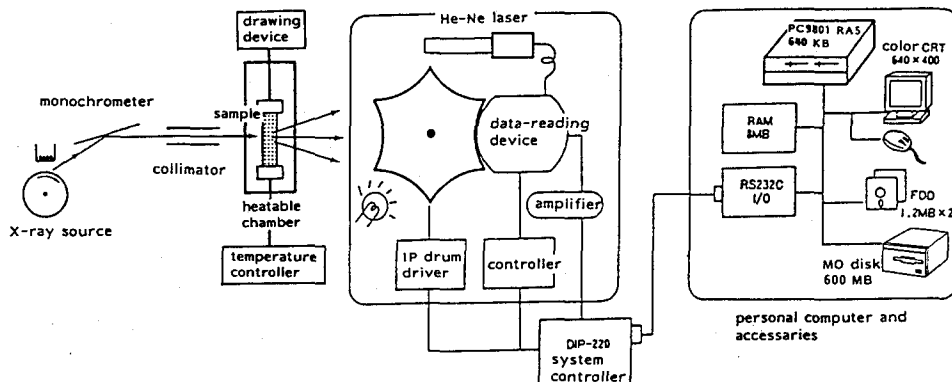


Fig. 2 Scheme of an X-ray diffraction system with IPs.

tube with the arm length of 150mm and attached in the way as shown in Fig. 1. The optical device slides from side to side parallel to the axle of the IP cassette as rotating. The tip of the tube runs colinearly to the concaved surface of IP with a clearance of 0.1mm. Laser beams are focused onto the IP with the diameter of 0.125mm, and hence, the IP is divided into pixels (image elements) with the size of 0.125 mm \times 0.125 mm. Divided by the pixel size, an IP of 200 mm \times 150 mm gives 3.87M intensity data. Intensity data thus accumulated are converted into digital values and stored in magneto-optical (MO) disk. The whole system is controlled by a personal computer (NEC PC-9801RA5), as mapped in Fig. 2.

Specimens

Ultra-high molecular weight polyethylene (UHMWPE) (Hizex Million M240 produced by Mitsui Petroleum Co. Ltd) was crystallized from the melt. The bulky sample was skived into thin sheets of the thickness of 0.5mm.

RESULTS AND DISCUSSIONS

Performance of IP

A pixel of IP stores the integrated intensity of the dynamic range up to 10^5 . X-ray films and an X-ray TV system response proportionally over the intensity range of only 2-3 orders of magnitude. The PSPC is a very sensitive detector and counts up to an intensity of 10^5 counts/sec without losses. However, a two-dimensional PSPC is severely limited only to measuring weak intensity. In contrast, since the IP covers the intensities of the dynamic range up to 10^5 over the whole area, it is superior to others as a two-dimensional recording medium of X-rays. However, the IP has a serious fault of aging; the excited phosphors decay with time. Figure 3 shows the intensities which were measured as a function of the lapse of time after irradiation. The intensity decreases rapidly within ten minutes after irradiation and gradually with time. The present system was designed to take up a time series of diffraction patterns while structural changes were in progress. It takes 5 min to read out a set of data from an IP. Since their intensity data are read out after six IPs are exposed, there is a time lag

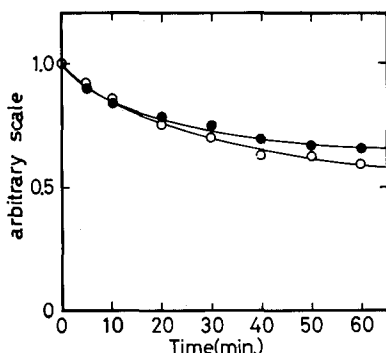


Fig. 3 Rate of the decay of excited IP as a function of the lapse of time after irradiation. Open and solid circles denote the results obtained from the intensity measurement of the 110 reflection of polyethylene with the different exposure time of 10 sec and 100 sec, respectively.

of about 30 min between readout from the first IP and that from the last one. The intensities recorded in the last IP decrease largely for the period of time, and hence, it makes no sense to compare quantitatively the absolute values of intensity among different plates. Further, the rate of decay is dependent of the initial intensity; the ratio of intensity at the lapse of time t to that at $t=0$ decreases slower for the higher initial intensity. Within the period of 30 min in question, however, the ratio may be regarded almost independent of the initial intensity. This implies that diffraction profiles are not so seriously deformed after ageing within the present period. Thus, we can quantitatively discuss the structural changes on the basis of results obtained by profile analysis.

Deformation process of UHMWPE

Figure 4 shows a time series of X-ray diffraction patterns of a UHMWPE sheet which were obtained using IPs with an exposure time of 10 sec while it was being drawn at room temperature at a rate of 5 cm/min. The patterns were processed with a personal computer to divide their intensities into several grades with different colors. Figure 5 shows the azimuthal intensity profiles smoothed by the least squares method; A corresponds to the profile of the orthorhombic 110 reflection¹⁵⁾ and B the 001 profile of the monoclinic phase.^{16,17)} From Figs. 4 and 5, we know the following interesting changes of diffraction patterns during drawing.

- 1) The orthorhombic 110 and 200 reflections, which are initially Debye-Sherrer rings, are gradually arc-shaped into seemingly a four-point pattern with drawing. Their intensity maxima move to the equator (the direction perpendicular to the drawing direction), but never converged on it even when the sample was drawn till it was broken at the draw ratio of about 4.
- 2) From the draw ratio of about 2, the diffuse orthorhombic 110 and 200 reflections are detectable on the equator. With further drawing, their intensities increase whereas the azimuthal reflections become weak.
- 3) As seen in Fig. 4, the monoclinic reflections appear at the draw ratio of about 1.2. Indexing is on the basis of the unit cell by Seto et al.¹⁷⁾ The intensity peak of the monoclinic reflection is first observed in the the drawing direction. The profile of monoclinic reflection is split into a four-point type, and the intensity maxima move toward the equator with further drawing.

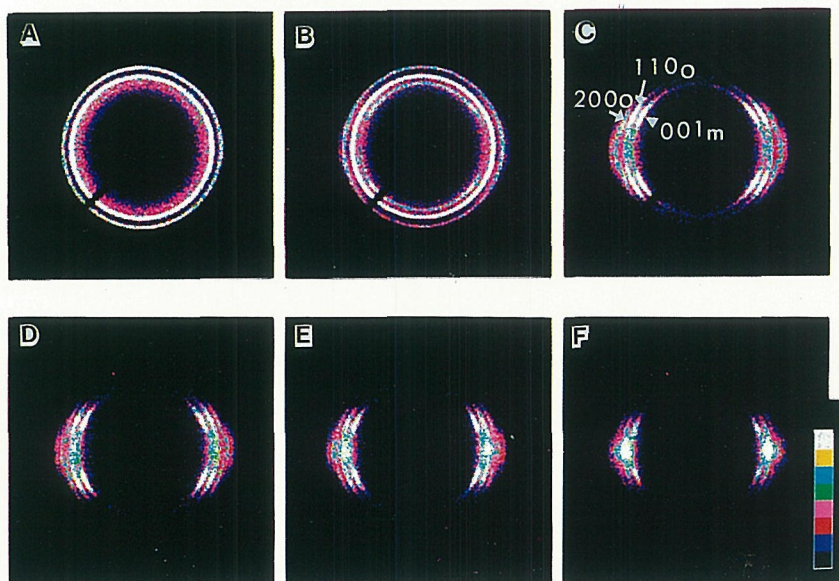


Fig. 4 Change of X-ray diffraction patterns during drawing at room temperature, photographed from the screen of color CRT. Draw ratio: 1.0(A), 1.25(B), 1.75(C), 2.25(D), 2.75(E) and 3.75(F). Drawing direction is vertical.

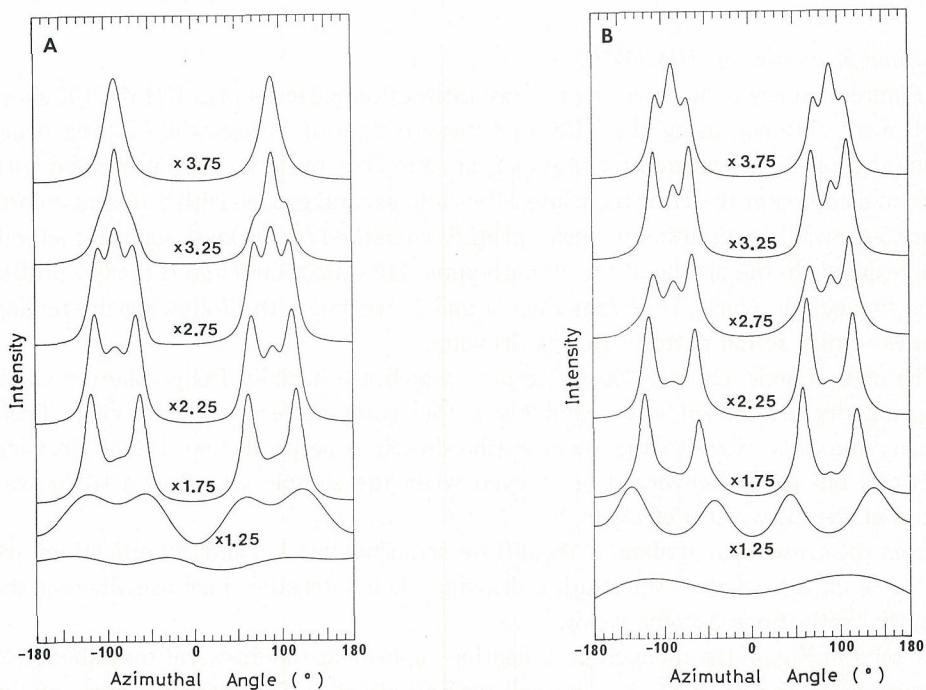


Fig. 5 Azimuthally scanned intensity profiles corresponding to Fig. 4, for (A) the 110 reflection of the orthorhombic phase and (B) the 001 reflection of the monoclinic phase. The angles of $\pm 90^\circ$ correspond to the direction perpendicular to the drawing direction.

In the case of high density polyethylene, the orthorhombic 110 and 200 reflections behave in a similar way by drawing at room temperature, and the monoclinic reflections are also produced transiently from an early stage of deformation as well and disappear in the fiber structure after necking.⁴⁾ In contrast, UHMWPE can never be drawn into a fiber structure at room temperature but broken. However, the fact that the orthorhombic 110 and 200 reflections are observed on the equator from an initial stage of drawing of UHMWPE shows that the fiber structure is partly given rise to in the sample, probable, by micro-necking. In these deformation behaviors, UHMWPE differs from high density polyethylene.

The drawing behavior largely depended on the drawing temperature. Figure 6 shows a series of X-ray diffraction patterns of UHMWPE which were taken while it was being drawn at 110°C. The corresponding azimuthal profiles of the orthorhombic 110 and 200 reflections are shown in Fig. 7. It is distinct from the drawing at room temperature in that in Fig. 6, the reflections due to the monoclinic phase are not seen. The monoclinic phase is produced by drawing at a temperature below about 85°C and not above the temperature. It is interesting that the temperature of 85°C corresponds to the temperature where the α_c -relaxation of polyethylene crystal takes place.¹⁸⁾ This does not always mean that the monoclinic crystals grown by stretching are transformed into the orthorhombic phase through the α_c -relaxation mechanism of molecular chains, because the monoclinic crystals produced at low temperatures do not disappear till it is heated up to about 110°C (the temperature is not uniquely fixed but depends on the degree of initial deformation).⁵⁾ Another distinction of Fig. 7 from Fig. 6 is in the behavior of the orthorhombic 110 and 200 reflections with drawing; first, the sample can be drawn into the fiber structure, and second, the 200 reflection converges onto the

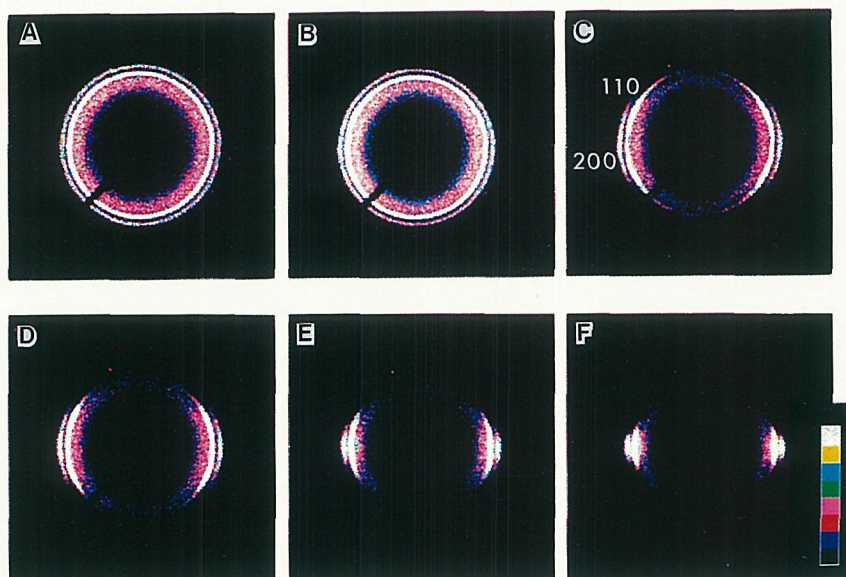


Fig. 6 Change of X-ray diffraction patterns of UHMWPE during drawing at 110°C, photographed from the screen of color CRT. Draw ratio; 1.0(A), 1.25(B), 1.75(C), 2.25(D), 2.75(E) and 3.75(F). Drawing direction is vertical.

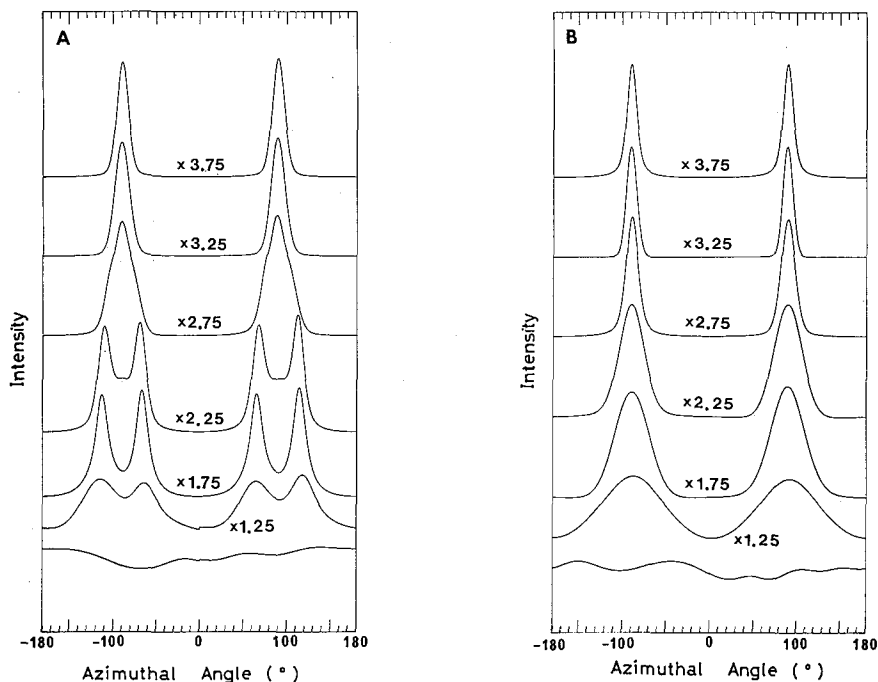


Fig. 7 Azimuthally scanned intensity profiles corresponding to Fig. 6, for the (A) 110 and (B) 200 reflections of the orthorhombic phase. The angles of 90° correspond to the direction perpendicular to the drawing direction. Figures in (A) and (B) denote the draw ratio.

equator at an early stage of drawing whereas the 110 reflection is retarded from converging, exhibiting the pattern like a four-point one.

Morphological changes of high density polyethylene spherulites, which take place when they are drawn at various temperatures, were detailed by electron microscopy by T. Nagasawa and K. Kobayashi.¹²⁾ When drawn at low temperatures, the spherulites are first broken at their lateral zones where lamellae oriented perpendicular to the drawing direction and their rupture extends in the direction of drawing through necking. By drawing at high temperatures, lamellae become separate at the lateral zones of spherulites, and slipping between lamellae is dominant in the longitudinal zone which is the part interposed between angles of $\pm 45^\circ$ with respect to the drawing direction. Thus, when polyethylene is drawn at high temperatures, the long axes of lamellae (the b-axis) of spherulites tend to be oriented preferentially parallel to the drawing direction through slipping between lamellae and rotation of lamellae around their long axis. Consequently, the a-axis orients quickly on the equator; the a-axis orientation occurs.¹⁰⁾ According to previous works with the extruded film, the film is abruptly extended into a fiber structure through necking without production of monoclinic crystals when drawn in the b-axis direction.^{4,19)} Thus, it is partly explained that no monoclinic crystals are given rise to by drawing lamellae in the b-axis direction at high temperatures, because the b-axis aligns parallel to the drawing direction at an early stage of drawing.

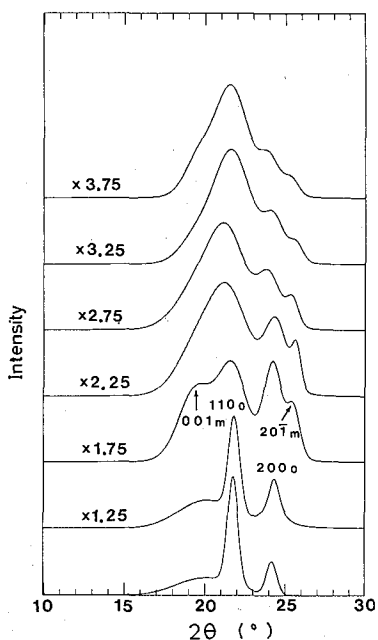


Fig. 8 Diffraction profiles scanned radially, i.e., in the horizontal direction of Fig.4.

Figure 8 shows the line profiles scanned in the direction normal to the drawing direction, i.e., the computer-processed intensity data of Fig.4 in the horizontal direction. The diffraction peaks of the orthorhombic reflections become broader with drawing, and due to overlapping of the monoclinic diffractions on them, the whole diffraction profile is complicated. We applied the least squares method to analyse the line profiles and obtained the lattice spacings from the peak maxima and the corresponding integral breadths.²⁰⁾ The changes in the (200) lattice spacing and its integral breadth are shown in Figs. 9(b), respectively. From these figures, we read following

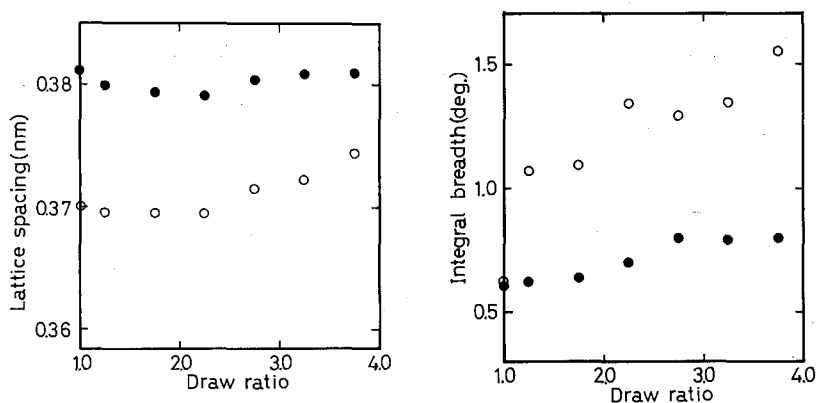


Fig. 9 (A) change in the (200) lattice spacing with the draw ratio. (B) change in the integral breadth of 200 reflection. No correction is done for the instrumental broadening. In both (A) and (B), open circles correspond to room temperature and solid circles to 110°C.

features; (1) the (200) lattice spacing increases largely from the draw ratio of about 2 and (2) correspondingly, the integral breadth increases. The 110 reflection also shows similar behaviors. These explain that the deformation of UHMWPE proceeds on drawing in the following manner; the lamellar crystals are destroyed and divided into crystallites with a smaller size and their lattice is expanded by introduction of distortions or defects.

CONCLUDING REMARKS

It is found that the newly constructed X-ray recording system with the IPs is useful to follow the process of the structural changes dynamically and quantitatively, when they do not proceed so quickly. Hopefully, it may be applied to a dynamic study on other structural changes such as solid-solid transition. Further, drawing contour maps of the diffraction patterns, though not exemplified here, we can know the details of the features of, say, diffuse scattering. However, in order to examine rapid structural changes on the basis of intensities, the rate of reading out intensity data from the IP should be increased.

REFERENCES

- (1) A. Kawaguchi, T. Ichida, S. Murakami and K. Katayama, *Colloid & polymer Sci.*, **262**,597(1984)
- (2) T. Ichida, M. Tsuji, S. Murakami, A. Kawaguchi and K. Katayama, *Colloid & Polymer Sci.*, **263**, 293(1985)
- (3) A. Kawaguchi, S. Murakami, K. Kajiwara, K. Katayama and D. Nerger, *J. Polymer Sci., Polymer Phys.*, **27**, 1463(1989)
- (4) K. Shimamura, S. Murakami and K. Katayama, *Bull. Inst. Chem. Res., Kyoto Univ.*, **55**, 269(1977)
- (5) A. Kawaguchi, S. Murakami, T. Ohta, M. Mihoichi and K. Katayama, The Proceeding of the 6-th Polymer Processing Society (Nice, France, April 17-20, 1990), 6, 6-05.
- (6) K. Takahashi, K. Kohda, J. Miyahara, Y. Kanemitsu, K. Amitani and S. Shionoya, *J. Luminescence*, **31&32**, 266(1984)
- (7) J. Miyahara and H. Kato, *Oyo Butsuri*(in Japanese), **53**, 884(1984)
- (8) J. Miyahara, K. Takahashi, Y. Amemiya, N. Kamiya and Y. Satow, *Nuclear Inst. Methods Phys. Res.*, **A246**, 752(1986)
- (9) K. Sasaguri, S. Hoshino and R. Stein, *J. Appl. Phys.*, **35**, 47(1964)
- (10) T. Oda, S. Nomura and H. Kawai, *J. Polymer Sci.*, **A3**, 1993(1965)
- (11) I. L. Hay and A. Keller, *Kolloid-Z.u.Z. Polymere*, **204**, 43(1965)
- (12) K. Kobayashi and T. Nagasawa, *J. Polymer Sci.*, **C(15)**, 163(1966)
- (13) N. A. J. M. van Aerle and A. W. M. Braam, *J. Appl. Cryst.*, **21**, 106(1988)
- (14) N. A. J. M. van Aerle and A. W. M. Braam, *Makromol. Chem.*, **189**, 1569(1988)
- (15) C. W. Bunn, *Trans. Faraday Soc.*, **35**, 482(1939)
- (16) H. Kiho, A. Peterlin and P. H. Geil, *J. Appl. Phys.*, **35**, 1599(1964)
- (17) T. Seto, T. Hara and K. Tanak, *J. J. Appl. Phys.*, **7**, 31(1968)
- (18) M. Takayanagi, K. Imada, A. Nogai, T. Tatsumi and T. Matsuo, *J. Polymer Sci.*, **C(16)**, 867(1967)
- (19) K. Kobayashi, in *Polymer Single Crystals*, P. H. Heil, Ed., Interscience, New York, 1963.
- (20) A. Kawaguchi, R. Matsui and K. Katayama, *Bull. Inst. Chem. Res., Kyoto Univ.*, **58**, 470(1980)